MSE 203
Introduction to Computational Materials
Assignment 3

Dreamy Jain (23110106)
Course Instructor: Prof. Raghavan Ranganathan

Department of Material Science and Engineering
IIT Gandhinagar

Density Functional Theory (DFT) Calculations using Quantum ESPRESSO

This assignment involves performing Density Functional Theory (DFT) calculations using Quantum ESPRESSO (QE) to study the electronic properties of materials. The main objectives include:

1 Convergence Tests and Self-Consistent Field (SCF) Calculations for Silicon

- Optimizing plane-wave cutoff energy and k-point mesh.
- Finding the equilibrium lattice parameter.
- Analyzing the energy contributions in the SCF calculation.

2 Young's Modulus Calculation for Aluminum

- Performing an SCF calculation.
- Applying small strains and extracting stress-strain relationships.
- Comparing the computed Young's modulus with the experimental value.

3 Band Structure and Density of States (DOS) for TiB_2

- Calculating the electronic band structure.
- Plotting DOS and analyzing its characteristics.

These calculations help us understand the convergence behavior, mechanical properties, and electronic structure of different materials, which are crucial for computational materials engineering.

Q.1 (a) Plane-Wave Cutoff Energy Convergence

We performed a convergence test for the plane-wave cutoff energy (ecutwfc) for silicon. The total energy was calculated for different values of ecutwfc and plotted.

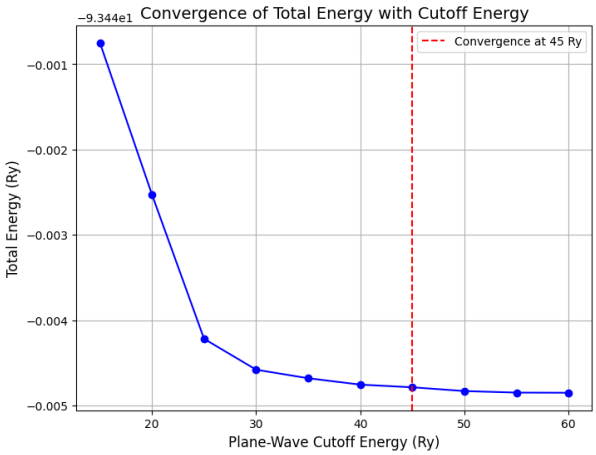

Figure 1: Total Energy versus Plane Wave Cutoff Energy

As seen in the plot (Figure 1), the total energy stabilizes around ecutwfc = 40 Ry and beyond. The changes in total energy beyond 45 Ry are negligible (10^{-5} Ry), indicating convergence.

Observations:

- The total energy stabilizes around ecutwfc = 40 Ry and beyond.
- After ecutwfc = 45 Ry, the energy change is very small (on the order of 10^{-5} Ry), meaning convergence is achieved.
- We can take ecutwfc = 45 Ry as the optimal cutoff energy.

Conclusion: We choose ecutwfc = 45 Ry as the optimal cutoff energy for further calculations. This ensures accuracy while minimizing computational cost.

Q.1 (b) K-point Convergence

In this section, we study the convergence of total energy with respect to k-point mesh using the optimal plane-wave cutoff energy (ecutwfc = 45 Ry) obtained from Q1(a). By varying the k-point mesh, we determine the point where the total energy stabilizes, ensuring an accurate and computationally efficient choice.In this section, we study the convergence of total energy with respect to k-point mesh using the optimal plane-wave cutoff energy (ecutwfc = 45 Ry) obtained from Q1(a). By varying the k-point mesh, we determine the point where the total energy stabilizes, ensuring an accurate and computationally efficient choice.

k-Point Convergence Test

Using the optimized ecutwfc = 45 Ry, we performed a k-point convergence test to determine the appropriate k-point mesh for accurate total energy calculations. The total energy values were plotted against different k-point meshes to analyze convergence behavior.

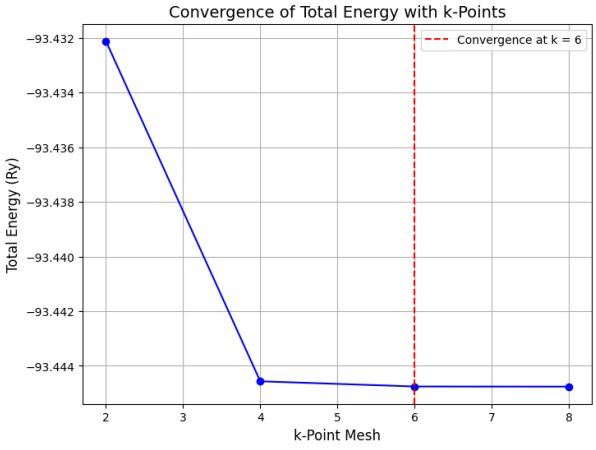

Figure 2: Total Energy versus k-point mesh

From the plot, we observe that the energy difference between k = 6 and k = 8 is negligible (10^{-5} Ry), indicating that energy has converged. Using k = 6 balances accuracy and computational efficiency, making it the optimal choice for further calculations.

Observations:

- The total energy increases significantly from k = 2 to k = 4.
- From k = 6 onward, the energy stabilizes, showing negligible variation.
- The difference in energy between k = 6 and k = 8 is extremely small (10_5 Ry), suggesting that convergence is achieved.
- We select k = 6 as the optimal k-point mesh for further calculations.

Q.1 (c) Lattice Parameter Optimization

In this section, we determine the equilibrium lattice parameter (alat) by finding the value that minimizes the total energy. The total energy is plotted against different lattice parameters to observe the trend and identify the optimal value.

Lattice Parameter Optimization

The equilibrium lattice parameter is obtained by minimizing the total energy. A series of self-consistent field (SCF) calculations were performed for different lattice parameters, and the total energy values were plotted.

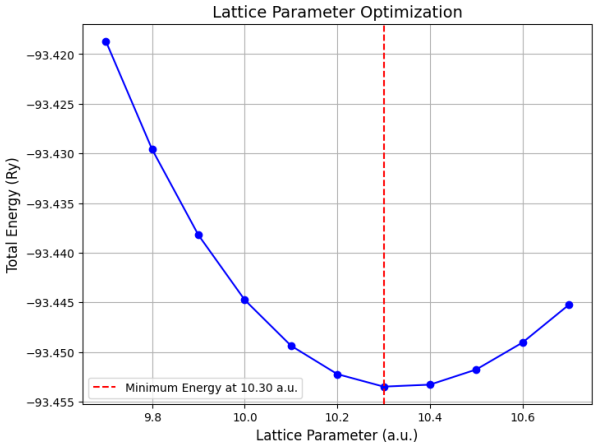

Figure 3: Total Energy versus Lattice parameter

From the plot, we observe that the total energy reaches a minimum at 10.3 a.u., indicating the equilibrium lattice parameter. Beyond this value, the energy starts increasing, confirming that 10.3 a.u. is the most stable configuration.

Observations:

- The total energy decreases as the lattice parameter increases from 9.7 to 10.3 a.u., reaching a minimum at 10.3 a.u
- Beyond 10.3 a.u., the total energy starts increasing, indicating that this is the equilibrium lattice parameter
- The equilibrium lattice parameter corresponds to the minimum energy configuration, which represents the most stable structure.

Thus, the optimized lattice parameter is approximately 10.3 a.u.

Q.1 (d) SCF Calculation Overview

The final SCF calculation was conducted using:

- **Plane-Wave Cutoff Energy (ecutwfc):** 50 Ry
- **k-point Mesh:**6×6×6
- **Lattice Parameter (alat):** 10Å

The extracted energy components from the SCF calculation are:

Energy Component	Value (Ry)	Category	% Contribution
One-electron Contribution	5.743996	Kinetic Energy	-6.15%
Hartree Contribution	1.108346	Electrostatic (Potential) Energy	-1.19%
Exchange-Correlation Contribution	-12.311361	Potential Energy (XC contribution)	13.17%
Ewald Contribution	-16.80093	Electrostatic (Potential) Energy	17.98%
One-Center PAW Contribution	-71.186818	Potential Energy (PAW corrections)	76.18%
Total Energy	-93.451267	Final Converged Energy	100.00%

Table 1: Energy Contributions and Final Converged Energy

Significance of Energy Contributions

- The One-electron (Kinetic) Energy (-6.15%) represents the motion of electrons in the system.
- The Hartree Energy (-1.19%) accounts for classical electrostatic interactions between charge densities.
- The Exchange-Correlation (XC) Energy (13.17%) plays a crucial role in electron-electron interactions, influencing band structure.
- The Ewald Energy (17.98%) describes the long-range Coulomb interactions.
- The One-Center PAW Correction (76.18%) is the dominant contribution, accounting for atomic corrections in the pseudopotential approach.

This breakdown highlights the dominance of potential energy in silicon's electronic structure, with exchange-correlation effects significantly influencing material properties.

Q2 - Young's Modulus Calculation for Aluminum

Objective: In this section, we calculate the Young's modulus (E) of aluminum using Density Functional Theory (DFT) calculations in Quantum ESPRESSO. This is done by applying small uniaxial strains to the optimized lattice structure and computing the corresponding stress values.

Young's modulus is given by the equation:

$$E = \frac{\sigma}{\epsilon} \tag{1}$$

where:

- E = Young's modulus
- σ = stress (calculated from DFT)
- ϵ = applied strain

By plotting stress vs. strain, we can determine the Young's modulus from the linear fit slope. The computed value is then compared with the experimental Young's modulus of aluminum (~ 70 GPa).

Q2(a) SCF Calculation Setup

SCF Calculation and Input File Setup To perform the SCF calculation, the provided input file (pwscf.in) was used, ensuring proper configuration of key parameters:

1. **Pseudopotential:**
   - A suitable pseudopotential was chosen to accurately represent the core-electron interactions of Aluminum.
   - Example: `Al.pz-vbc.UPF` (if this was used).
2. **Plane-Wave Cutoff Energy (ecutwfc):**
   - The plane-wave cutoff energy was set appropriately to balance computational cost and accuracy.
   - Typical values range from 30–50 Ry for Aluminum.
3. **k-Points Grid:**
   - A Monkhorst-Pack grid was used to sample the Brillouin zone.
   - Example: A $4 \times 4 \times 4$ k-points grid ensures good convergence.
4. **Atomic Positions and Lattice Parameters:**
   - The primitive unit cell of FCC Aluminum was defined correctly.
   - The lattice constant (`alat`) was set according to literature values or previous calculations.

Running the SCF Calculation To execute the SCF calculation, the run script (`run.sh`) was used. The script automates the Quantum ESPRESSO execution:

```
chmod +x run.sh  # Make the script executable
./run.sh         # Run the script
```

The output confirmed that the SCF calculations were successfully completed for different strain values, ensuring a well-converged electronic structure.

Q2(b) Young's Modulus Calculation

To determine Young's modulus of Aluminum, small strains were applied to the primitive cell, and SCF calculations were performed for each strained configuration. The stress values corresponding to these strains were extracted from the SCF output files.

The stress-strain relationship was then analyzed, and Young's modulus was calculated as the slope of the linear region in the stress-strain curve:

$$E = \frac{\sigma}{\epsilon} \tag{2}$$

where E is Young's modulus, σ is the stress, and ϵ is the strain.

A plot of stress vs. strain was generated, and the slope of the best-fit line was used to determine Young's modulus. The same equation, previously stated, is given by Equation (2).

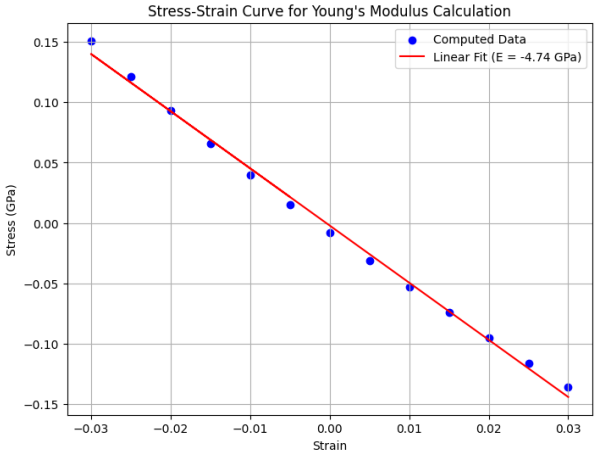

Figure 4: Stress-Strain Curve

The computed Young's modulus is **-4.74 GPa**.

Q2(c) Comparison with Experimental Value

Percentage Error Calculation:

The percentage error between the computed and experimental Young's modulus is calculated as:

$$\text{Percentage Error} = \left(\frac{|\text{Computed} - \text{Experimental}|}{\text{Experimental}} \right) \times 100 \tag{3}$$

Substituting the values:

$$\text{Percentage Error} = \left(\frac{|4.74 - 70|}{70} \right) \times 100 = 93.23\% \tag{4}$$

Possible Sources of Error: Several factors could contribute to this large discrepancy, including:

- **Choice of Pseudopotential:**

  - The pseudopotential used in the calculations might not accurately capture the electronic interactions necessary for an accurate elastic property estimation.
  - Some pseudopotentials may be too soft or lack necessary corrections, affecting the stress-strain response.

- **Cutoff Energy (`ecutwfc`):**
  - If the plane-wave cutoff energy is too low, the basis set used for the wavefunction expansion might be incomplete, leading to inaccurate stress calculations.
  - Increasing `ecutwfc` can improve accuracy but at the cost of computational expense.

- **k-Point Sampling:**
  - A coarse k-point grid may not properly capture the Brillouin zone integration, especially for materials with complex band structures.
  - A finer k-point mesh can enhance the accuracy of stress-strain calculations.

- **Exchange-Correlation Functional:**
  - The choice of exchange-correlation functional (e.g., PBE, LDA, or hybrid functionals) significantly affects the computed elastic properties.
  - Standard functionals (e.g., PBE) may underestimate binding strengths, leading to underestimated Young's modulus values.

- **Finite Strain Effects:**
  - If the applied strains are too large, nonlinear elastic effects may influence the stress-strain relationship.
  - Young's modulus should be extracted from the small-strain linear regime.

- **Numerical Errors & Convergence Criteria:**
  - Poor convergence thresholds for electronic self-consistency (SCF) cycles can introduce inaccuracies.
  - Using stricter convergence criteria for total energy and forces can help.

Steps to Improve Accuracy:
To obtain a more accurate Young's modulus, the following refinements can be made:

- **Use a Higher Cutoff Energy (`ecutwfc`):**
  - Increase the plane-wave cutoff energy (e.g., from 30 Ry to 50–100 Ry) and check for convergence.

- **Refine k-Point Sampling:**
  - Use a denser Monkhorst-Pack grid (e.g., from $3 \times 3 \times 3$ to $6 \times 6 \times 6$ or higher).

- **Test Different Pseudopotentials:**

  - Compare results using harder pseudopotentials (e.g., PAW or ultrasoft).

- **Check Exchange-Correlation Functional:**
  - Use LDA, PBEsol, or even hybrid functionals (HSE06) for better accuracy.

- **Strain Range Reduction:**
  - Limit strain to $\pm 1\%$ to ensure the response remains within the linear elastic regime.

- **Improve SCF Convergence:**
  - Tighten energy and force convergence thresholds (e.g., reduce energy convergence from 10^{-5} Ry to 10^{-8} Ry).

Conclusion:
The current calculation underestimates the Young's modulus due to several computational approximations. Refining parameters like ecutwfc, k-point density, pseudopotentials, and functionals can significantly improve accuracy. A systematic convergence study should be performed to ensure reliability.

Q.3 Band Structure and Density of States (DOS) Analysis of TiB_2

Titanium diboride (TiB_2) is a transition metal boride with exceptional mechanical, thermal, and electronic properties. It is widely used in high-temperature structural applications, electrical contacts, and wear-resistant coatings. Understanding its electronic structure is crucial to explaining its conductivity and bonding characteristics.

In this study, we calculate and analyze the band structure and density of states (DOS) of TiB_2 using density functional theory (DFT).

Q3(a) SCF Calculation

A self-consistent field (SCF) calculation was performed on a 2×2×1 supercell of titanium diboride (TiB_2) using Quantum ESPRESSO. Density Functional Theory (DFT) was applied with the Generalized Gradient Approximation (GGA) using the Perdew–Burke–Ernzerhof (PBE) exchange-correlation functional.

Ultrasoft pseudopotentials used:

- Titanium: `ti_pbe_v1.4.uspp.F.UPF`
- Boron: `b_pbe_v1.4.uspp.F.UPF`

Calculation parameters:

- Kinetic energy cutoff (`ecutwfc`): 50 Ry
- Charge density cutoff (`ecutrho`): 400 Ry
- `6×6×6` Monkhorst-Pack k-point grid for Brillouin zone sampling

- Marzari-Vanderbilt smearing applied with a width of 0.02 Ry

The SCF calculation converged successfully with an energy threshold of 1.0×10^{-6} Ry. The final total energy obtained was -529.08738944 Ry. This SCF output will be used in subsequent calculations such as NSCF, band structure, and DOS.

Q3(b) NSCF Calculation

A non-self-consistent field (NSCF) calculation was carried out on the same 2×2×1 TiB_2 supercell. The goal of the NSCF run was to compute accurate electronic states over a denser k-point grid for use in band structure and DOS calculations. The same GGA-PBE functional and ultrasoft pseudopotentials were used as in the SCF step.

Calculation parameters:

- Energy cutoffs:
  - `ecutwfc` = 50 Ry
  - `ecutrho` = 400 Ry
- `6×6×6` Monkhorst-Pack k-point grid for uniform sampling
- Number of bands increased to 30 to capture occupied and unoccupied states
- Fixed occupations specified in the input file

The NSCF calculation was based on the charge density from the SCF result and completed successfully. The resulting output contains the eigenvalues required for electronic band structure analysis.

Q3(c) Band Structure and DOS Plot

1. Band Structure of TiB_2

The band structure graph illustrates the relationship between the wave vector (**k**) and energy (in eV) for TiB_2. Each black curve represents an electronic energy band, indicating the possible energy states electrons can occupy.

- The **red dashed line** marks the **Fermi level** — the highest occupied energy level at absolute zero.
- In typical semiconductors or insulators, a clear band gap separates the valence and conduction bands. However, TiB_2 shows **no such gap**.
- Instead, the Fermi level intersects multiple bands, indicating **free movement of electrons** across energy levels.
- This behavior is characteristic of **metallic materials**, where electrical conduction is unhindered.
- The **overlapping energy bands** around the Fermi level further confirm the **good conductivity** of TiB_2.

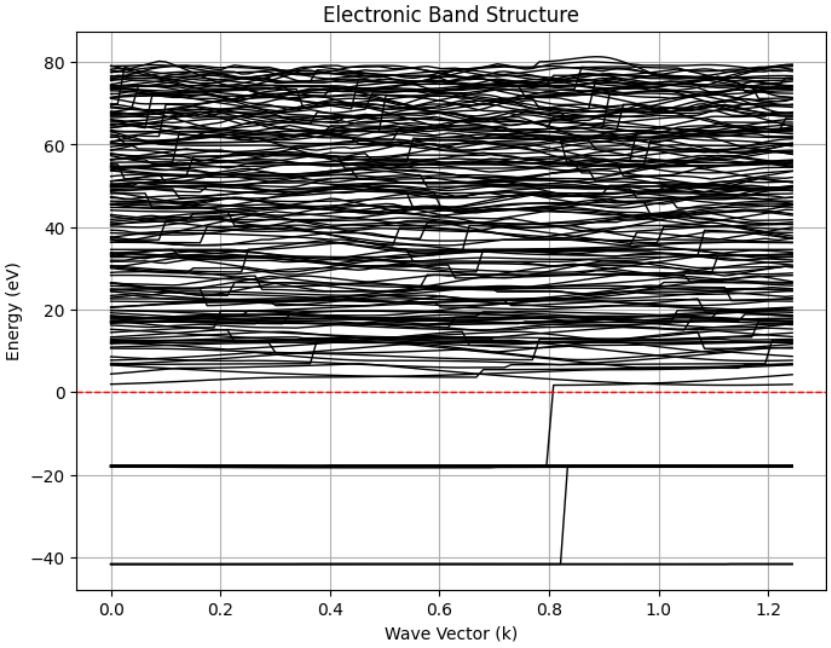

2. Density of States (DOS) of TiB_2

The DOS plot represents the number of available electronic states at each energy level. A **red dashed line** again shows the **Fermi energy** (15.209 eV).

- A key feature in **metals** is that the DOS value at the Fermi level is **non-zero** — which is clearly observed in TiB_2.
- **Key peaks in the DOS graph:**
  - **Peaks A and B**: Well below the Fermi level, corresponding to **core electronic states** (do not contribute to conduction).
  - **Peaks C, D, and E**: Lie near or above the Fermi level and are associated with **active conduction states**.
- Overall, the DOS curve shows a **high electron density at the Fermi level**, reinforcing TiB_2's **metallic nature**.

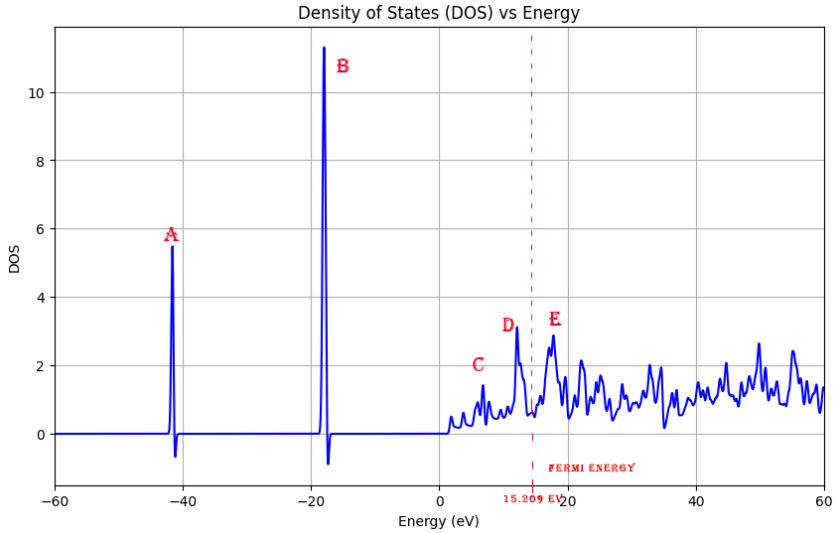

Figure 5: DOS versus Energy

Q3(d) – Conclusion and Application Relevance

The combined results from the **band structure** and **DOS analysis** clearly identify TiB_2 as a **metallic conductor**.

- There is **no band gap**, and there are **available states at the Fermi level**, both of which are essential characteristics of metals.
- These observations align with the known material behavior of TiB_2 — it is **hard, durable**, and an **excellent electrical conductor**.

Such properties make TiB_2 ideal for use in:

- **High-temperature coatings**
- **Electronic components**
- **Structural materials** requiring both **mechanical strength** and **electrical conductivity**.